Supplement of Clim. Past, 17, 1507–1521, 2021
https://doi.org/10.5194/cp-17-1507-2021-supplement

Climate of the Past
Open Access
EGU

Supplement of

The atmospheric bridge communicated the δ^{13}C decline during the last deglaciation to the global upper ocean

Jun Shao et al.

Correspondence to: Jun Shao (junshao@usc.edu)

cGENIE $\delta^{13}C_{(DIC)}$ tracer decomposition and attribution error analysis

Model summary and primary tracer overview

We employ the open source intermediate complexity Earth system model cGENIE.muffin (DOI:10.5281/zenodo.4903423) to decompose the different components comprising the stable carbon isotopic ($\delta^{13}C$) composition of dissolved inorganic carbon (DIC) in the ocean. As implemented here, cGENIE comprises: (1) a 3D ocean circulation model component configured on a 36×36 equal are grid, with 16 non-equally spaced vertical levels in the ocean, (2) a 2D energy-moisture balance model ('EMBM') component, and (3) a 2D dynamic-thermodynamic sea-ice model component. The absence of a dynamical atmospheric GCM component then requires that (fixed, annual average) 2D fields of wind stress and speed are applied, which are re-gridded from observations, plus a zonally-average profile of planetary albedo is applied. Greenhouse gas feedback on climate is implemented by applying a top of the atmosphere anomaly in radiative forcing according to the relative deviation of atmospheric CO_2 from a reference value of 278 ppm. These three individual components, their coupling, plus details of the simplified atmospheric component and associated climate feedbacks, are described in *Marsh et al.* [2011] (and references therein).

The basic physics parameter calibration of the climate model component is as per *Cao et al.* [2009]. Our implementation of cGENIE includes a relatively complete description of the cycling of carbon and oxygen in the ocean plus exchange with the atmosphere, as described in *Ridgwell et al.* [2007] and *Cao et al.* [2009]. In addition, the carbon isotopic (both $\delta^{13}C$ and radiocarbon ($\Delta^{14}C$)) composition of all the carbon pools plus associated fractionations are represented, as described in *Ridgwell et al.* [2007] with additional description and evaluation in *Kirtland Turner and Ridgwell* [2016].

In addition to basic carbon (DIC and $\delta^{13}C_{(DIC)}$), alkalinity, single nutrient (PO_4), oxygen (and sulphate) cycling in the model, we include a variety of diagnostic tracers to decompose all of the 'components' of DIC and its $\delta^{13}C$ signature. (Note that the tracer notation given here follows that of the model and associated documentation, and can deviate from that of the main paper. Equivalents are given when needed.) These explicitly simulated tracers are:

- Preformed DIC ($DIC_{(pref)}$) and preformed $\delta^{13}C_{(pref)}$.
  The values of these tracers are reset to the respective concentrations of DIC and $^{13}C_{(DIC)}$ at the ocean surface at each time-step, and thereafter are carried conservatively (no loss of gain of carbon can occur) by ocean circulation.
- Regenerated DIC from organic matter, $DIC_{(Csoft)}$ (also known as 'C_{soft}'), and its associated isotopic signature ($\delta^{13}C_{(Csoft)}$).
  In this, the value of these tracers is reset to zero at the ocean surface at each time-step. In the ocean interior, respired carbon (and for $\delta^{13}C_{(Csoft)}$, the ^{13}C component of respired carbon) associated with remineralization of both particulate and dissolved organic matter is added to the tracer field. The tracer fields are also subject to ocean circulation.
  Note that because isotopes are carried explicitly as concentrations in cGENIE (and

delta (δ) values only generated in conjunction with bulk concentrations for results output), the $\delta^{13}C_{(Csoft)}$ tracer is simulated as a concentration and exactly as per $DIC_{(Csoft)}$ and does not need to be e.g. normalized to a fractional contribution to $\delta^{13}C_{(DIC)}$ (as is required e.g. for the AOU-derived tracer, described subsequently).

- Preformed O_2 ($O_{2(pref)}$).
  The value of this tracer is reset to the concentration of dissolved O_2 at the ocean surface at each time-step, and thereafter carried conservatively (no loss of gain of dissolved oxygen can occur) by ocean circulation.
- Preformed PO_4 ($PO_{4(pref)}$).
  The value of this tracer is reset to the concentration of dissolved PO_4 at the ocean surface at each time-step, and thereafter carried conservatively (no loss of gain of dissolved phosphate can occur) by ocean circulation.

The final component of DIC – carbon released through the dissolution of $CaCO_3$ in the water column (and released from the upper sediments) – $DIC_{(CaCO3)}$ – is calculated by difference (of DIC vs. $DIC_{(pref)}$ plus $DIC_{(Csoft)}$) and is not simulated here explicitly as a separate tracer. (Ditto for $\delta^{13}C_{(CaCO3)}$.)

Steady state experiment description and basic tracer analysis

We start by performing a decomposition analysis of the carbon components, using a standard preindustrial configuration of cGENIE (*Cao et al.* [2009]) that is run for 10,000 years to steady-state. The results of this are shown broken down by basin as zonally-averaged concentrations shown in Figure S2. Notable here is the relatively insignificant contribution of $DIC_{(CaCO3)}$, particularly in the upper ca. 1000 m of the water column, where it typically contributes no more than about 10 μmol kg^{-1} DIC. (This will be important later in justifying the various assumptions inherent in the AOU-based analysis of the LOVECLIM experiment.)

In Figure S3, we show the corresponding basin zonal means of $\delta^{13}C_{(DIC)}$ simulated by cGENIE in the preindustrial ocean, together with the 3 components that contribute to the net distribution. Notable again here is the weak contribution that can be ascribed to the dissolution of $CaCO_3$. Indeed, in the upper ca. 1000 m of the water column, the (positive) contribution of $\delta^{13}C_{(CaCO3)}$ is generally less than about 0.05‰, compared to a contribution from $\delta^{13}C_{(Csoft)}$ that can exceed (in magnitude) -2.0‰ and to a $\delta^{13}C_{(pref)}$ contribution lying between ca. 1.5 and 2.5‰. Note the different (to $\delta^{13}C_{(Csoft)}$) color scale for $\delta^{13}C_{(CaCO3)}$ and that the surface (and convected-to-depth in the North Atlantic) apparent high values (purple colors) are an artifact of the differencing of DIC and $^{13}C_{(DIC)}$ concentrations used in calculating $\delta^{13}C_{(CaCO3)}$ (i.e. at close-to-zero values for $DIC_{(CaCO3)}$ spurious apparent isotopic values can arise).

In a final, simple numerical check of this diagnostic tracer scheme (not shown), we re-run the 10,000 year preindustrial experiment but with the production of $CaCO_3$ at the ocean surface disabled, i.e. in the complete absence of any $\delta^{13}C_{(CaCO3)}$ component to $\delta^{13}C_{(DIC)}$. From this we confirm, as expected, that $DIC = DIC_{(pref)} + DIC_{(Csoft)}$, and $\delta^{13}C_{(DIC)} = \delta^{13}C_{(pref)} + \delta^{13}C_{(Csoft)}$ to within 0.03‰. That this error is not zero to within numerical precision, is due to the specific numerical scheme and implementation of the preformed and regenerated tracers in cGENIE. As described in the main text, for the preformed tracers, an anomaly is applied to each preformed tracer at the ocean surface at each time-step, equal to the difference between the current bulk tracer

value and the preformed tracer value (as opposed to simply directly setting the values equal in the code). Because in the numerical scheme, all fluxes, including those induced by ocean circulation and any preformed tracer anomalies, are calculated simultaneously and only summed and applied to update the tracer concentration field at the very end of the model time-step, preformed tracer concentrations at the ocean surface and at the end of the time-step, never exactly equal those of the bulk tracer. The maximum error (ca. -0.03‰) occurs at the surface of the Southern Ocean as a result of the energetic ocean transport environment (principally, convection) there. This error is propagated throughout the ocean, creating a mean ocean net error of -0.012‰ in the diagnostic tracer scheme.

Summary of calculated 'derived' tracers

Although LOVECLIM is able to simulate preformed PO_4(P_{pref}) and hence calculate regenerated PO_4 by differencing with (total) [PO_4], and then to C_{soft} by scaling with a P:C ratio – see Menviel et al. [2015]), LOVECLIM was not run with this tracer included in the published deglacial experiment used in this study. Instead, C_{soft} in LOVECLIM must be estimated from apparent oxygen utilization (AOU) (for example, as applied to output from the Bern3D model in Menviel et al. [2015]). To quantify the errors inherent in this approach, we calculate a number of derived tracer fields based on the primary (simulated) ones:

1. $O_{2(sat)}$ – O_2 solubility at every ocean grid point using ambient temperature and salinity values (plus density, ρ). For this, we calculate the solubility coefficient (α, mol kg^{-1} atm^{-1}) for O_2 following Wanninkhof (1992) and using the coefficients from *Millero and Sohn* [1992], and assume an atmospheric partial pressure for oxygen (pO_2) of 0.2096 atm:
   $O_{2(sat)} = \rho \times \alpha \times pO_2$
   (This diagnostic employs the exact same calculation as used 'normally' in cGENIE for simulating air-sea gas exchange (Ridgwell et al., 2007).)
2. AOU – calculated as the difference between $O_{2(sat)}$ and the actual model simulated tracer field of [O_2]:
   $O_{2(AOU)} = O_{2(sat)} - [O_2]$
3. AOU-P – regenerated PO_4 – estimated from AOU divided by the assumed cGENIE O_2:P Redfield ratio of (-)138:1:
   $P_{(AOU)} = O_{2(AOU)} / 138$
   Note that for the purposes of this analysis, we ignore complications caused by the occurrence of sulphate reduction in oxygen minimum zones, meaning that locally, there will be a 'missing' fraction of regenerated phosphate that is not associated with AOU. For reference, the global oxygen consumption associated with particulate organic carbon oxidation in the preindustrial experiment is 608 Tmol O_2 yr^{-1}, while (in the absence of nitrate reduction) while the global rate of SO_4^{2-} consumption is 29 Tmol SO_4^{2-} yr^{-1} (equivalent to 58 Tmol O_2 yr^{-1}). However, this does not equate to a ~10% global error in estimating AOU-P, because the re-oxidation of H_2S consumes dissolved oxygen, closing the AOU budget. Rather, the impact of not accounting for SO_4^{2-}/H_2S transformations will be a pattern of positive and negative error in estimating regenerated PO_4 from AOU.

4. AOU-DIC – DIC regenerated from organic matter – estimated from AOU-P multiplied by the assumed cGENIE P:C Redfield ratio of 1:106:
   $DIC_{(AOU)} = 106 \times P_{(AOU)}$
   This is an estimate of C_{soft}.
5. AOU-$\delta^{13}C$ – the $\delta^{13}C$ contribution of DIC from regenerated from organic matter – estimated by weighting the $\delta^{13}C$ of POC exported from the overlying ocean surface ($\delta^{13}C_{(Corg)}$) by the fractional contribution of AOU-DIC to (total) DIC:
   $\delta^{13}C_{(AOU)} = \delta^{13}C_{(Corg)} \times DIC_{(AOU)}/DIC$
   This is an estimate of $\delta^{13}C_{(Csoft)}$.
6. C_{soft}-$\delta^{13}C$ – the $\delta^{13}C$ contribution of DIC from regenerated from organic matter – estimated by weighting the $\delta^{13}C$ of POC exported from the overlying ocean surface by the fractional contribution of C_{soft} to (total) DIC:
   $\delta^{13}C_{(Csoft)'} = \delta^{13}C_{(Corg)} \times DIC_{(Csoft)}/DIC$
   This is an alternative estimate of $\delta^{13}C_{(Csoft)}$ that is independent of the assumptions inherent in AOU. It also acts as a test of the assumption that one can tag regenerated carbon ($DIC_{(Csoft)}$) with the isotopic signature of POC exported from the overlying ocean in order to estimate regenerated $\delta^{13}C$. Note that this post-processed diagnostic ($\delta^{13}C_{(Corg)}$-prime) is distinct from the explicitly simulated $\delta^{13}C_{(Csoft)}$ tracer (see description of primary tracers).

For completeness, we also simulate but do not report, $P_{(pref)}$, and from this derive regenerated P ($P_{(Csoft)}$) and hence can obtain a second alternative estimate of the $\delta^{13}C$ contribution of DIC from regenerated from organic matter ($\delta^{13}C_{(Csoft)''}$).

All outputs are calculated on the basis of annual mean values of the 3D ocean tracer fields.

Steady state analysis of the errors inherent in estimating C_{soft}-$\delta^{13}C$

We start our derived tracer analysis by illustrating the errors inherent in AOU itself. As is widely appreciated, AOU overestimates the consumption of oxygen through respiration as a consequence of incomplete equilibrium occurring between the ocean surface and overlying atmosphere which causes $O_{2(sat)}$ to be an overestimation of real ocean oxygenation. There is also an estimation error due to the non-linear solubility of oxygen, which follows a quasi-exponential decay with increasing temperature. This results in an *underestimate* of AOU, because $O_{2(sat)}$ is underestimated when calculated from the ambient (linear mixing) temperature of parcel of water derived from sources equilibrated at 2 (or more) different sea surface temperatures. Figure S4 shows the difference between AOU and 'true' oxygen utilization (TOU), with the latter calculated as the difference between preformed [O_2] ($O_{2(pref)}$) and simulated ambient [O_2]. From this it is clear that the disequilibrium error dominates, with the surface overestimate in AOU and its propagation into the ocean interior being particularly pronounced at high southern latitudes. While cGENIE calculates an AOU error about 30% smaller than originally reported by *Ito et al.* [2004] using the MIT OGCM, our results fall between the range of the different (higher resolution) models presented by *Duteil et al.* [2013]. The zonal patterns calculated by cGENIE (Figure S4) are also similar to the Atlantic and Pacific sections presented in both papers (*Ito et al.* [2004], *Duteil et al.* [2013]).

Converting AOU to AOU-C (the AOU-derived estimate of respired carbon – see above), translates to an error (overestimate) in C_{soft} of around 30 μmol kg^{-1} and which dominates all of the deep Pacific and Indian Ocean below about 1000 m (Figure S6). (In cGENIE, the North Atlantic Ocean surface is closer to equilibrium and full oxygenation and hence creates a plume of relatively low DIC error waters along the path of North Atlantic deep water.) However, we find that the $\delta^{13}C$ error – the difference between explicitly simulated $\delta^{13}C_{(Csoft)}$ and the AOU-based estimation (AOU-$\delta^{13}C$), deviates noticeably from the pattern of the DIC error (Figure S5, 2nd row down). Specifically: while the largest error in $\delta^{13}C_{(Csoft)}$ is indeed found throughout the depth water column in the Southern Ocean, following the error in AOU and the C_{soft} field derived from this, the mid and low latitudes are characterized by much reduced error in $\delta^{13}C_{(Csoft)}$ and deviate from the pattern of DIC error (top row). Somewhat enigmatically, a prominent $\delta^{13}C_{(Csoft)}$ error maximum is also found throughout much of the water column in the North Pacific (but not at the northern-most end of the Indian Ocean). We resolve this by differencing AOU-$\delta^{13}C$ (#5) and C_{soft}-$\delta^{13}C$ (#6), whereby the error associated with assuming a fixed value field of $\delta^{13}C_{(POC)}$ cancels out, leaving only the error in deriving C_{soft} from AOU. This $\delta^{13}C$ error field (Figure S5, 2nd row from bottom) now visually correlates much more closely with the AOU DIC error field (top row). The 2nd component to the total AOU based C_{soft}-$\delta^{13}C$ error can be calculated as the difference between 'true' (explicitly simulated) C_{soft}-$\delta^{13}C$, and C_{soft}-$\delta^{13}C$ estimated from $DIC_{(Csoft)}$ together with $\delta^{13}C_{(POC)}$ (#6). This is shown in the final row of Figure S5. Here, it can be seen that a significant positive error arises at mid-to-low latitude in the ocean subsurface.

What this analysis reveals is a flaw in how C_{soft}-$\delta^{13}C$ is being estimated by convoluting a field of exported $\delta^{13}C_{(POC)}$ with C_{soft}. The 'true' C_{soft}-$\delta^{13}C$ tracer field is not only a product of local DIC release (from organic carbon remineralization) with its associated local isotopic value ($\delta^{13}C_{(POC)}$), but also how the composition of a parcel of water is transformed as it moves through the deep ocean. The C_{soft}-$\delta^{13}C$ tracer field is hence an integrated history of isotopic remineralization, just as C_{soft} is an integrated history of bulk carbon remineralization. Importantly, in the real ocean, and to some extent simulated in many models including cGENIE, $\delta^{13}C_{(POC)}$ varies significantly spatially: from values less than (more negative) than -30‰ towards the poles, to more (less negative) than -20‰ at the equator. Hence, tagging an equatorial subsurface parcel of water with an equatorial-only $\delta^{13}C_{(POC)}$ value omits the history of that water mass that will have started at high latitudes where initially it receives a much more isotopically depleted remineralized carbon input. Notably and rather more by luck than design, models either assuming a fixed fractionation of POC $\delta^{13}C$ vs. DIC $\delta^{13}C$, or like LOVECLIM, otherwise producing a relatively small pole-to-equator gradient in POC $\delta^{13}C$, will be subject to only a small associated error in convoluting exported $\delta^{13}C_{(POC)}$ with C_{soft} (and leaving the related error related to the AOU approximation dominant everywhere).

Transient* C_{soft}-$\delta^{13}C$ *error analysis

So far, we have considered only a steady-state situation and the question arises: what happens during climate and carbon cycle change – do the error fields change and relatively by how much? For the final part of our diagnostic tracer framework analysis we turn to a simple transient simulation. For this, we take the same model preindustrial steady state, but apply

(and hold) a radiative forcing at the top of the atmosphere equivalent to a doubling of atmospheric pCO_2 (to 556 ppm). The actual value of pCO_2 simulated in the model is free to vary in response to the applied surface warming, but this does not affect the imposed radiative forcing. (Note that no injection of carbon to the atmosphere is used to induce the warming, and both bulk and ^{13}C carbon inventories are conserved between ocean+atmosphere as compared to the preindustrial spin-up.) The evolution over 2000 years of key global mean atmospheric and climate variables, along with mean ocean $\delta^{13}C_{(DIC)}$, $\delta^{13}C_{(pref)}$, and $\delta^{13}C_{(Csoft)}$, are shown in Figure S6. We pick 2 contrasting time-horizons to focus our final tracer analysis on: (1) 200 years, which corresponds in terms of time, to the 'rapid' interval from 16.3-16.1 ka of atmospheric $\delta^{13}C$ decline recorded in ice-cores (and coincidently corresponds to the interval of most rapid $\delta^{13}C_{(pref)}$ and $\delta^{13}C_{(Csoft)}$ change in our simple experiment), and (2) 2000 years, which approximately corresponds to the overall 17.2 to 15 ka early deglaciation interval. Note that imposing enhanced radiative forcing on a preindustrial state is not meant to replicate deglaciation. Rather, we deliberately create as simple a transient climate and carbon cycle change as possible for the purpose of assessing non steady-state diagnostic tracer behavior. However, although the warming does approximately correspond in overall magnitude to that associated with deglaciation and is additionally associated with reorganization of the Atlantic Meridional Overturning Circulation as per the delgaciation, it should also be noted that this idealized instantaneous-perturbation transient experiment is distinct from the deglacial-like experiment described and analyzed in the main text.

Figure S7 shows the change in $\delta^{13}C_{(DIC)}$ as compared to a control (continuing preindustrial) experiment for year 200 (top) and 2000 (2nd-from-top row). In this specific idealized cGENIE model experiment, the patterns of change in $\delta^{13}C_{(DIC)}$ are dominated by changes in nutrient re-supply to the ocean surface, and hence the strength of the biological export from the surface and organic matter remineralization in the ocean interior – all in turn reflected in changes in $\delta^{13}C_{(Csoft)}$ (not shown). In contrast, changes in $\delta^{13}C_{(pref)}$ (not shown) are largely confined to the upper ca. 1000 m as a result of CO_2 outgassing as the ocean warms. We also calculate how the error in $\delta^{13}C_{(Csoft)}$ as estimated from AOU changes – shown in the 2nd-from-bottom and bottom rows of Figure S7 for year 200, and 2000, respectively. We find that the isotopic error across the uppermost ca. 500 m depth in the model hardly changes as compared to the control (the close-to-zero anomaly values in Figure S7) and after 2000 years, as the system starts to re-establish a steady state, the spatial distribution of the error anomaly largely follows that of the steady state AUO error (SI Figure 4).

cGENIE* C_{soft}-$\delta^{13}C$ *analysis summary

Relevant to the LOVECLIM model analysis conducted in the paper, we can conclude the following from the above experiments and analysis:

i. With a relatively minimal latitudinal gradient in the $\delta^{13}C$ signature of exported POC in LOVECLIM, the error in estimating $\delta^{13}C_{(Csoft)}$ and hence the relative contribution of $\delta^{13}C_{(Csoft)}$ vs. $\delta^{13}C_{(pref)}$ to a given simulated $\delta^{13}C_{(DIC)}$ change in LOVECLIM, will be dominated primarily by the error in estimating C_{soft} from AOU. (cGENIE, in contrast, sees approximately equivalent-in-magnitude error terms due to both error sources throughout the low and mid latitudes – Figure S5.)

ii. At least in the context of the idealized transient experiment tested here, the AOU-induced $\delta^{13}C_{(Csoft)}$ error is almost invariant throughout the uppermost ca. 500 m of the ocean (Figure S7). This is likely simply because the AOU error in $\delta^{13}C_{(Csoft)}$ is close to zero in this region of the ocean to start with (Figure S5) and that AOU provides a relatively reliable means of estimating C_{soft} here. The important point is that this is close to the depth range where planktic and (most) shallow benthic foraminifera are sampling the isotopic composition of DIC.

References:

Cao, L., Eby, M., Ridgwell, A., Caldeira, K., Archer, D., Ishida, A., Joos, F., Matsumoto, K., Mikolajewicz, U., Mouchet, A., Orr, J. C., Plattner, G.-K., Schlitzer, R., Tokos, K., Totterdell, I., Tschumi, T., Yamanaka, Y., and Yool, A.: The role of ocean transport in the uptake of anthropogenic CO_2, 6, 375–390, https://doi.org/10.5194/bg-6-375-2009, 2009.

Duteil, O., Koeve, W., Oschlies, A., Bianchi, D., Galbraith, E., Kriest, I., and Matear, R.: A novel estimate of ocean oxygen utilisation points to a reduced rate of respiration in the ocean interior, Biogeosciences, 10, 7723–7738, https://doi.org/10.5194/bg-10-7723-2013, 2013.

Kirtland Turner, S. and Ridgwell, A.: Development of a novel empirical framework for interpreting geological carbon isotope excursions, with implications for the rate of carbon injection across the PETM, Earth and Planetary Science Letters, 435, 1–13, https://doi.org/10.1016/j.epsl.2015.11.027, 2016.

Ito, T., Follows, M. J., and Boyle, E. A.: Is AOU a good measure of respiration in the oceans?: AOU AND RESPIRATION, 31, n/a-n/a, https://doi.org/10.1029/2004GL020900, 2004.

Marsh, R., Müller, S. A., Yool, A., and Edwards, N. R.: Incorporation of the C-GOLDSTEIN efficient climate model into the GENIE framework: "eb_go_gs" configurations of GENIE, Geosci. Model Dev., 4, 957–992, https://doi.org/10.5194/gmd-4-957-2011, 2011.

Menviel, L., Mouchet, A., Meissner, K. J., Joos, F., and England, M. H.: Impact of oceanic circulation changes on atmospheric $\delta^{13}CO_2$: $\delta^{13}CO_2$, 29, 1944–1961, https://doi.org/10.1002/2015GB005207, 2015.

Ridgwell, A., Hargreaves, J. C., Edwards, N. R., Annan, J. D., Lenton, T. M., Marsh, R., Yool, A., and Watson, A.: Marine geochemical data assimilation in an efficient Earth System Model of global biogeochemical cycling, 4, 87–104, 2007.

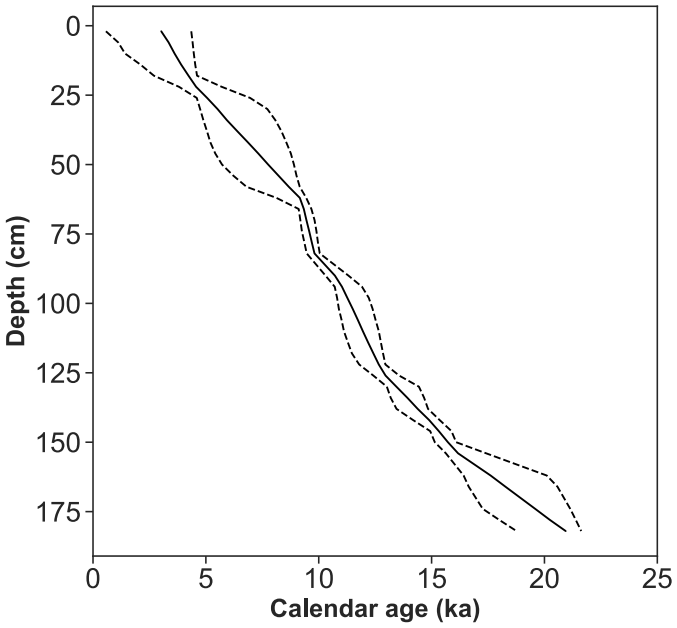

Figure S1. Age model of GeoB17402-2. The dash lines represent 2.5% and 97.5% quantile of the assigned ages.

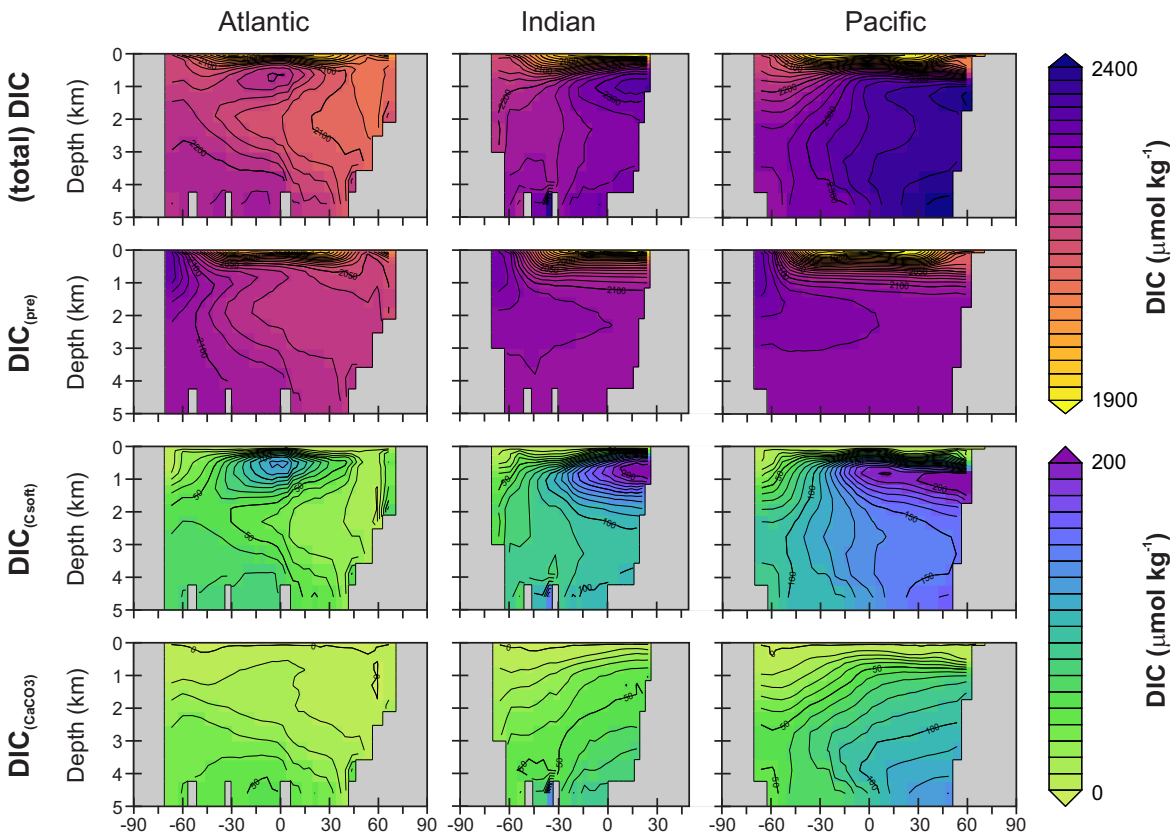

Figure S2. cGENIE preindustrial steady state, mean annual zonally averaged, DIC, DIC_{pref}, DIC_{soft} and DIC_{caco3} distributions.

300

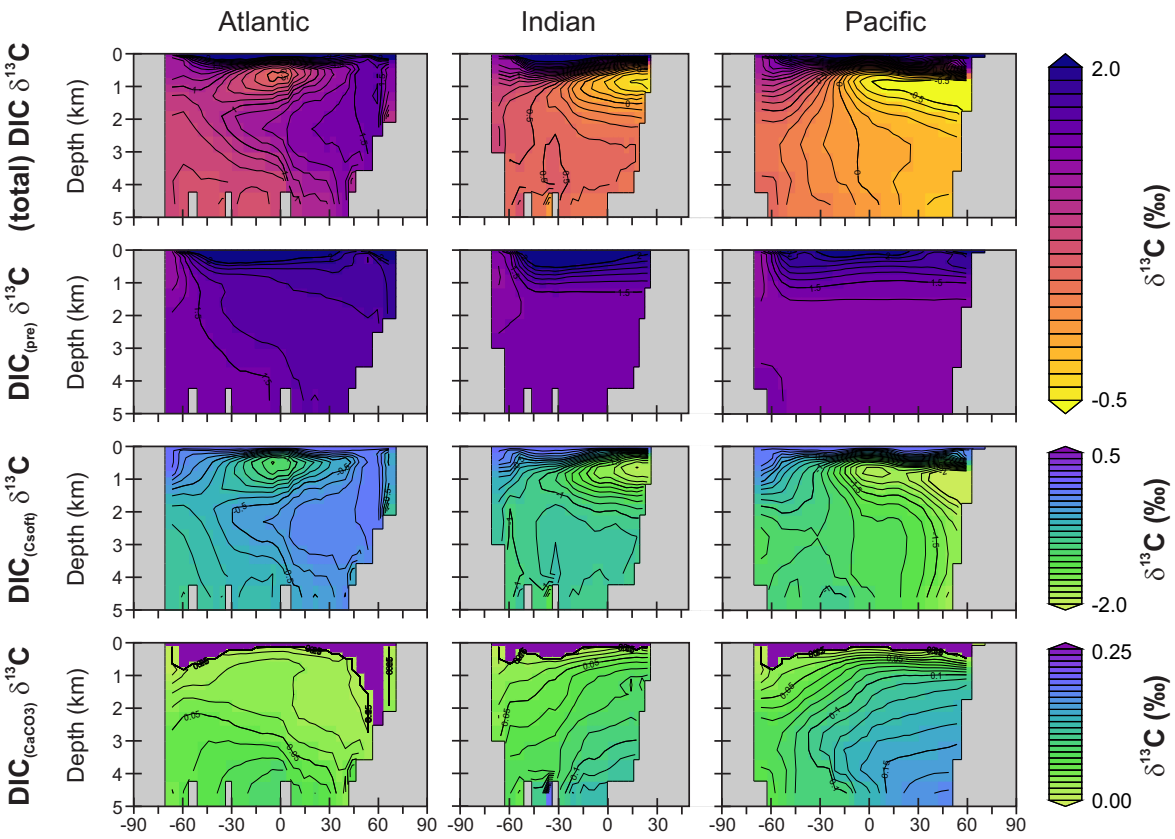

Figure S3. cGENIE preindustrial steady state, mean annual zonally averaged, distributions of the $\delta^{13}C$ of DIC, DIC_{pref}, DIC_{soft} and DIC_{caco3}.

305

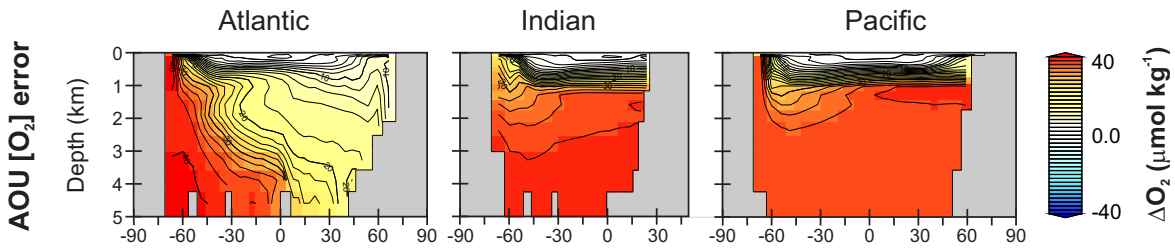

Figure S4. cGENIE preindustrial steady state AOU error analysis.

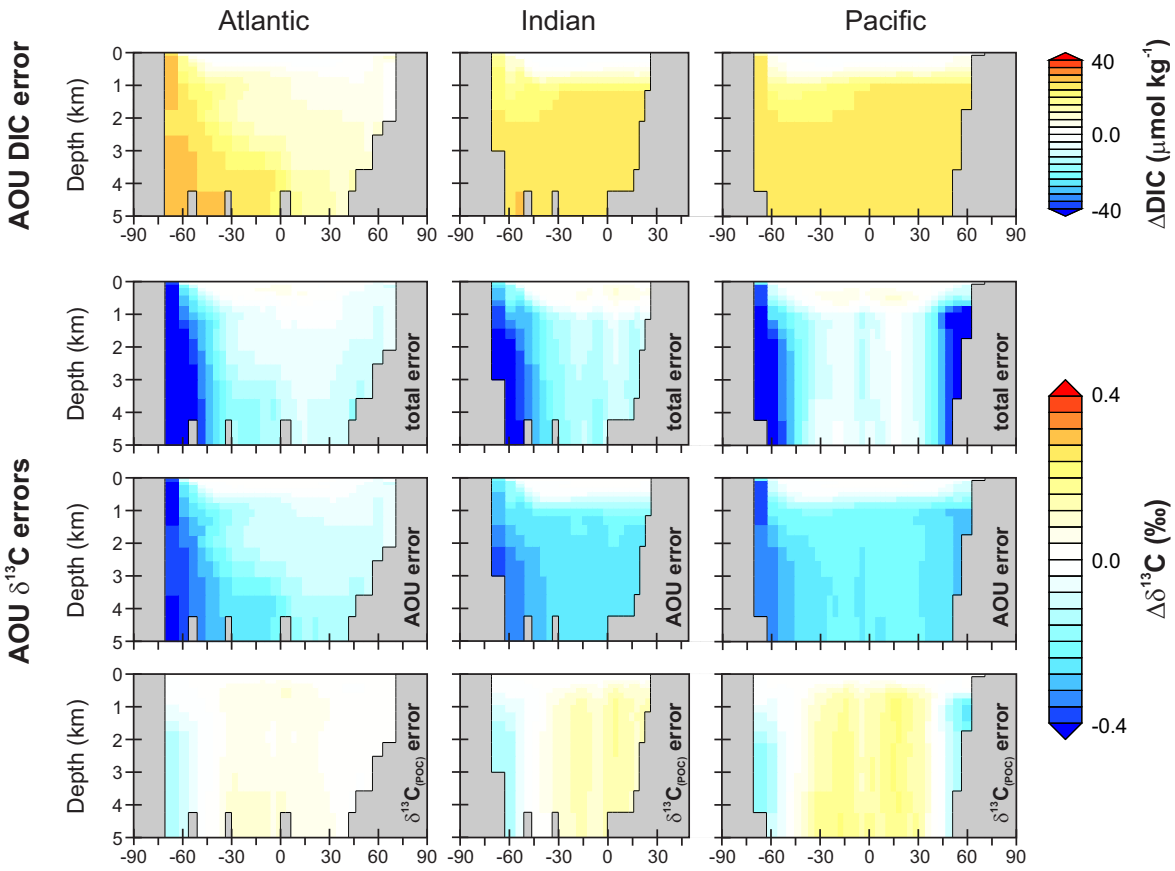

310

Figure S5. cGENIE preindustrial steady state AOU-based DIC and $\delta^{13}C$ error analysis.

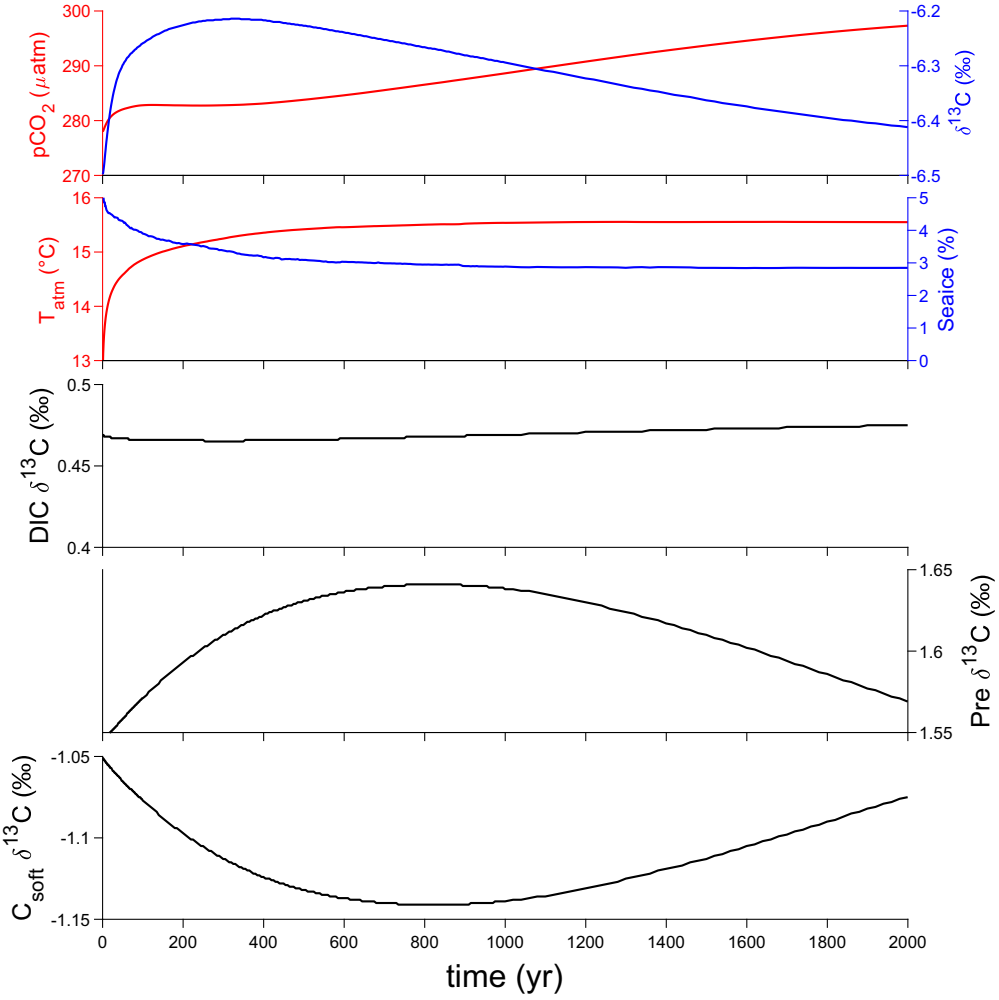

Figure S6. Time-series of cGENIE 2000-year idealized transient experiment.

315

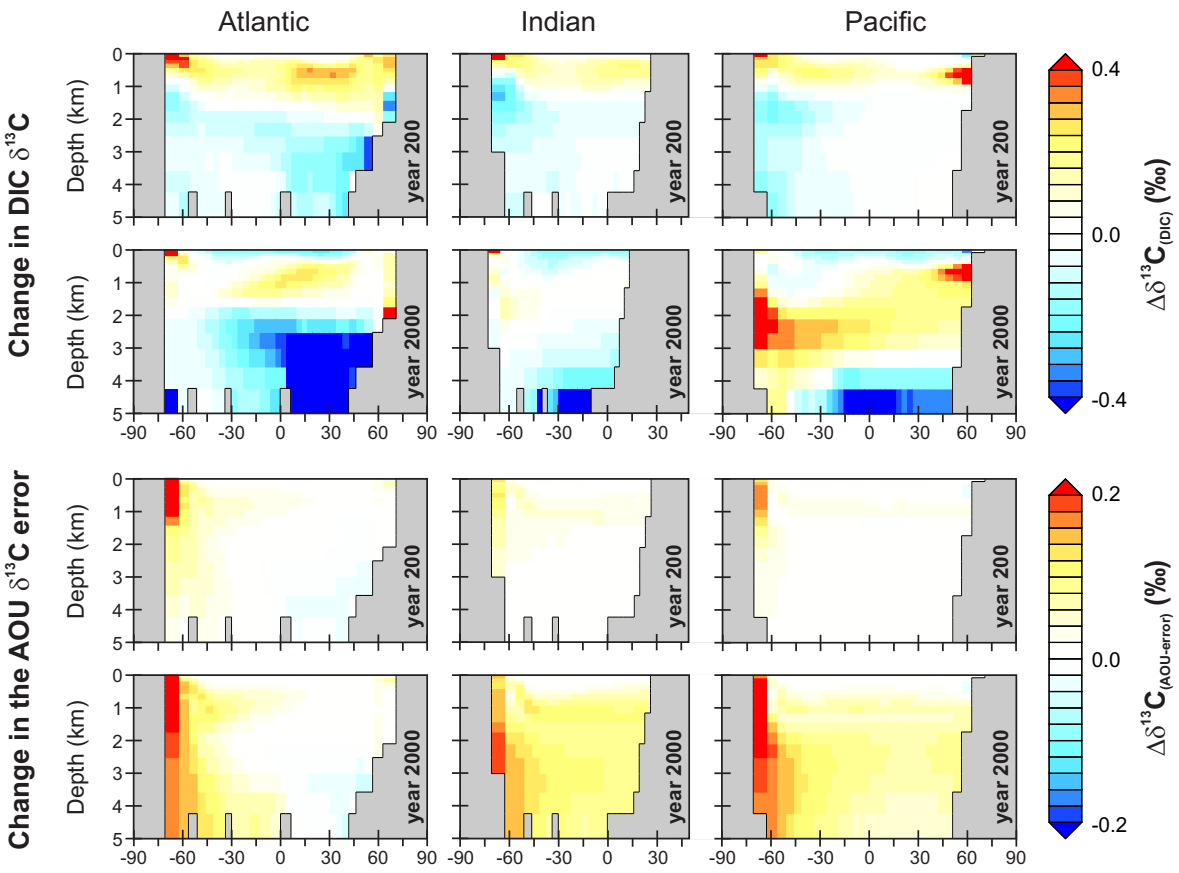

Figure S7. cGENIE 2000-year idealized transient experiment AOU error analysis.

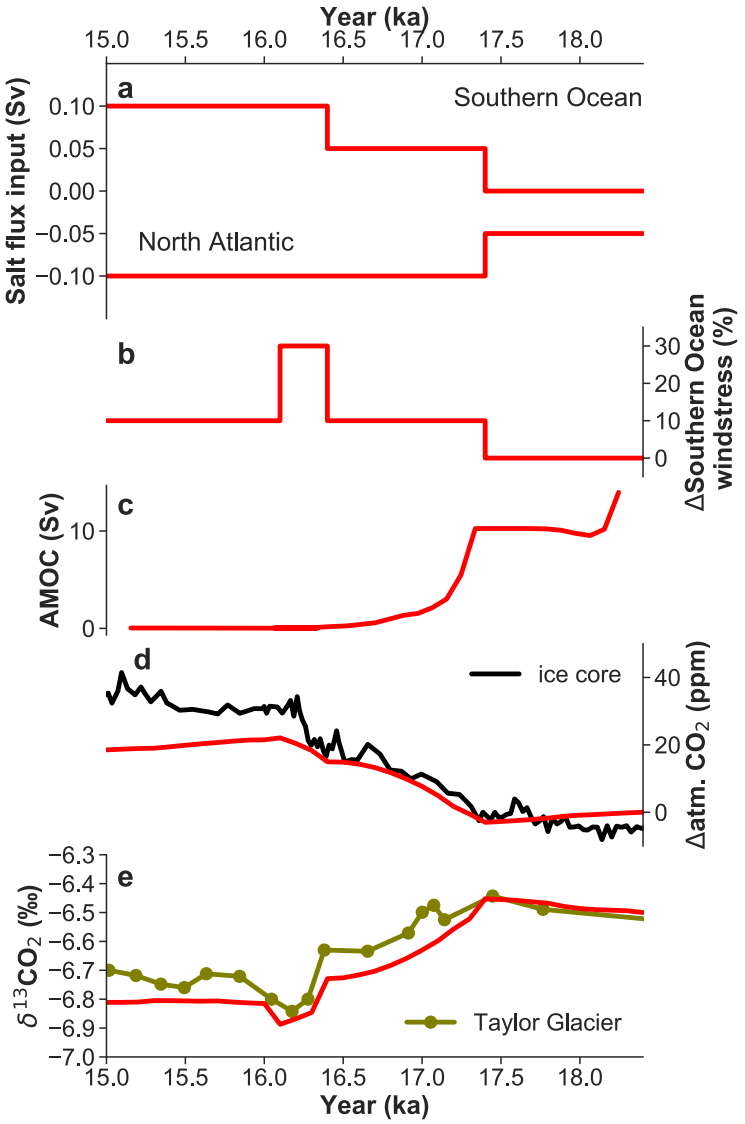

320

Figure S8. Forcing and atmospheric response in the cGENIE deglacial transient experiment.

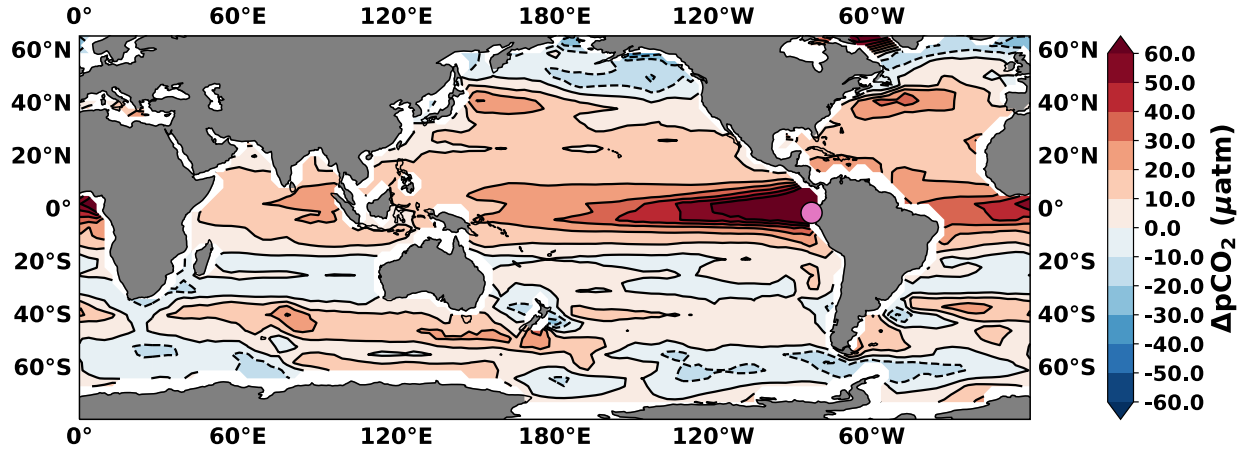

Figure S9. Air-sea pCO_2 gradient at 16 ka (i.e. Heinrich Stadial 1) simulated by LOVECLIM. The site of ODP 1238 is marked as a magenta circle.

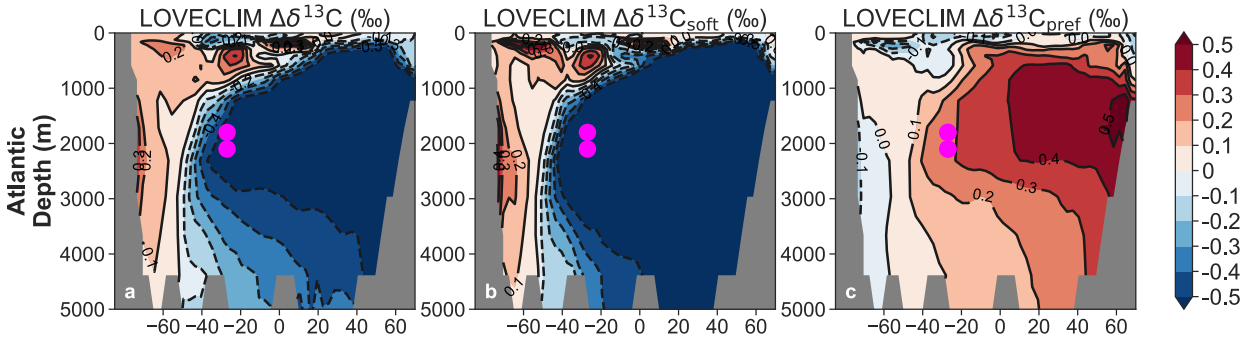

Figure S10. Atlantic zonal mean (60°W-10°W) anomalies (15ka minus 17.2ka) as simulated in LOVECLIM. The magenta circles mark the 78GGC and the 33GGC site.